

# ***Hypersonic Aerothermodynamics Methodology using ZONAIR for RLV/TPS Design and Analysis***<sup>+</sup>

P.C. Chen, D.D. Liu, K.T. Chang, X.W. Gao, and L. Tang  
ZONA Technology\*, Scottsdale, AZ, [www.zonatech.com](http://www.zonatech.com)

## ***Abstract***

*With continuing AFRL contractual support, the development of ZONA unified hypersonic/supersonic/subsonic aerodynamic method ZONAIR and its integration into ZONA aerothermoelastic software system including ASTROS for the thermal protection system (TPS) of RLV design/analysis was proven a successful tool. Substantial effort has been directed towards further development of a new module ZSTREAM and using it with ZONAIR to replace the outdated streamline modules in SHVD, thus to couple them with SHABP for aerothermoelastic applications. Feasibility cases studied included a CKEM body, blunt cones and a simplified X-34 wing-body. The cases selected are well validated with finite-difference solutions using CFL3D. Computed heat rates by applying ZONAIR with ZONA aerothermoelastic software to X-34 through two assigned hypersonic trajectories were found to agree well with those using MINIVER. A prototypical TPS subsystem was constructed using the obtained heat rates from X-43 as the input to the developed automated optimization module MINIVER/OPT for TPS sizing. With its FEM/TRIM modules ASTROS yields the trim solution and stress distribution for a flexible X-34 at a typical trajectory point, demonstrating the multifunctionality in the MDO capability for the present aerothermoelastic methodology.*

*Recent advances in the development of ZONAIR are reported. These include: (a) Development of an optimization procedure for TPS sizing using MINIVER with an innovative complex variable differentiation (CVD) scheme for sensitivity, i.e., the MINIVER/OPT module ;(b) Temperature mapping capability from aerodynamic to structural grids to account for the effect of aerothermoelasticity; and (c) Demonstration of automated mesh/panel generation capability and the design-oriented feature of AML coupling with ZONAIR*

## ***Background***

NASA's space launch initiative (SLI) has two emerging programs - the Orbital Space Plane and Next Generation Launch Technology programs. In response to these programs, it is required to identify technologies needed to create a new, safe, cost-effective launch system thus to generate an integrated technology plan. More urgently, it is required to develop and integrate maturing technologies in key areas, such as hypersonic aerodynamics/aeroheating, propulsion, structures and integrated vehicle systems preferably in a multidisciplinary design/analysis optimization (MDO) manner. NASA is currently working in concert with Department of Defense initiatives on a variety of launch system technologies including the design methodology development of a viable reusable launch vehicle (RLV).

Such a reusable launch vehicle (RLV)[1], during the course of its hypersonic re-entry/maneuver phases, will encounter an extreme environment with substantial aeroheating, which will generate thermal loads that would cause structural deformation of the RLV, while interacting with external hypersonic flow. This is known as the aerothermoelastic problem in hypersonic flight. *The present project is a result of continuing support of AFRL for the further development of an expedient hypersonic aerothermodynamic/aerothermoelastic methodology for the design/ analysis of RLV with its thermal protection system (TPS).* [2]

---

<sup>+</sup> Presented at NASA 14<sup>th</sup> Thermal Fluids Analysis Workshop 2003, August 18-22, 2003, Hampton, VA.

\* ZONA Technology, Inc. · 7430 E. Stetson Dr. Ste 205, Scottsdale, AZ 85251 · Tel (480) 945-9988 · Fax (480) 945-6588  
[www.zonatech.com](http://www.zonatech.com), [info@zonatech.com](mailto:info@zonatech.com)

## ***Introduction***

For RLV design consideration, it requires the synergic interdisciplines of hypersonic aerothermodynamics and aeroelasticity. In particular, the aerothermoelastic effects will strongly affect its thermal protection system (TPS)[3], hence the integrated RLV/TPS structural design. Therefore, for RLV/TPS design consideration, it requires a methodology for accurate aerothermodynamic-loads and aeroelastic-loads prediction to couple with an optimization method in order to achieve a viable RLV/TPS structural design with minimum weight objective. Toward this end, it is desirable to achieve, in an MDO procedure, an optimum TPS structural design, while performing the primary structure sizing so that the TPS design can augment the primary load bearing structure to satisfy all structural constraints including the aerothermoelastic constraint.

To develop a comprehensive aerothermoelastic program for RLV/TPS design requires careful planning of the required disciplines. It appears that thus far all required disciplines have been developed individually to a large extent including the trajectory analysis, the TPS sizing analysis, the thermal/structure analysis and the aerodynamic/aerothermodynamic programs. Thus, to integrate these programs into an efficient MDO procedure is a challenging task. Because the disparate analysis disciplines and their adopted methodologies being at different levels, these programs could not readily constitute a viable RLV/TPS design process. There are many stumbling blocks in achieving this integration task. For example, the low computational efficiency of the high fidelity aerodynamics/surface temperatures would prevent sufficient iterations in the design cycles. The interface between the surface temperature calculations and the structural heat transfer appears to be underdeveloped. Note that the temperature calculation is driven by trajectory analysis and high-fidelity aerodynamic computation, whereas the structural heat transfer analysis is driven by the thermal properties of the TPS and primary structure. Finally, the primary structural loads must be kept synchronized with the structural temperature distributions in order to ensure the primary structure is capable of bearing the in-flight launch loads and re-entry/maneuver loads.

Therefore, for an expedient integrated aerothermodynamics/aerothermoelastic design methodology we realize that a unified hypersonic panel method [4] with high-fidelity aerodynamic surface-compliant panels must be employed. Thus, these panels could be tightly coupled with a structural FEM (Finite Element Method) module such as ASTROS\* (Automated STRuctural Optimization Systems) [5], or NASTRAN for aerodynamic/structural interface in order to ensure a proper MDO procedure. For further advancement of the software architecture, the proposed integration of AML [6] with the aerothermoelastic program based on a high-fidelity panel aerodynamic methodology is mandatory. This will probably rule out the existing efficient but non-FEM compatible types of aerodynamic prediction programs such as APAS, Datcom, or AP98 [7, 8, 9]. On the other hand, any high-level CFD method would not be suitable as a rapid design tool under the proposed environment. Clearly, for an expedient, high-fidelity aerothermoelastic/aerothermodynamic program, a compatible hypersonic aerodynamic methodology is warranted. In the next section, we identify such a unified hypersonic panel method program is in fact the ZONAIR aerodynamic code [10].

Finally, ZONAIR in the hypersonic aerothermodynamics/aerothermoelastic MDO program will be integrated in a feature-based design environment using Adaptive Modeling Language (AML) [6] with parametric control of models and data exchange capability.

In the course of the development, our specific objectives include: (i) Establish interfaces between all key analysis software tools of the preliminary software system (see Fig 1) and (ii) Validate the proposed software system by a feasibility study on a selected RLV configuration (*e.g.*, X-34). In what follows, we will discuss the total integration program architecture, the central MDO methodology ASTROS and down to each disciplinary domains with separate case validations. Emphasis is placed on the recent development of a) temperature mapping capability from aerodynamic to structural grids and b) an automated TPS optimization scheme using MINIVER [11].

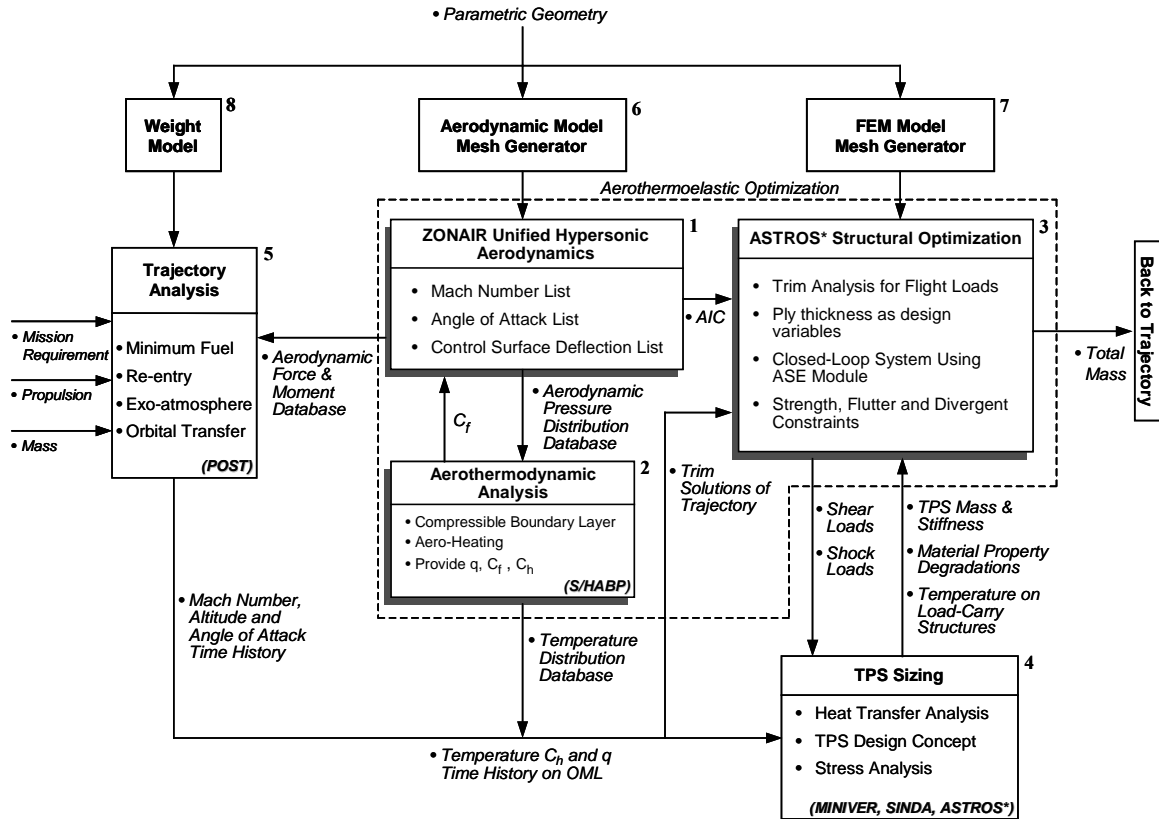


Fig 1 Block Diagram of Integrated Hypersonic Aerothermoelastic Program Architecture

### ZONAIR for Expedient Hypersonic Aerodynamics

For the defined comprehensive multidisciplinary design/analysis optimization (MDO) development involving aerothermodynamics, we propose the ZONAIR code for expedient hypersonic aerodynamic methodology [10]. ZONAIR is a high-fidelity unstructured panel code that is unified in subsonic, sonic, supersonic and hypersonic Mach numbers. Given flight conditions, ZONAIR, will provide aerodynamic pressures/forces/magnitudes generator to efficiently create aerodynamic and loads databases for 6DOF simulation and critical loads identification. ZONAIR is formulated based on the unstructured surface panel scheme that is compatible to the finite element methods. This enables the direct adoption of off-the-shelf finite element pre- and post-processors such as PATRAN, I-DEAS, FEMAP, etc. for ZONAIR panel model generation (see Figure 2). The specific capabilities of ZONAIR include:

- A unified high-order subsonic/supersonic/hypersonic panel methodology as the underlying aerodynamic force generator.
- Unstructured surface panel scheme compatible to the finite element method.
- Direct adoption of off-the-shelf FEM pre- and post-processors for rapid panel model generation.
- High quality streamline solution with a hypersonic boundary layer method for aerothermodynamics.
- Vortex roll-up scheme for high angle-of-attack aerodynamics.
- Trim module for flexible loads and aeroheating module for aeroheating analysis.
- Pressure interpolation scheme for transonic flexible loads generation.
- Aerodynamic and loads database for 6 d.o.f. simulation and critical loads identification.

ZONAIR consists of many submodules for various disciplines that include (1) AIC matrix generation module, (2) 3-D spline module, (3) Trim module, (4) Aeroheating module, (5) Vortex roll-up module and (6) Aerodynamic stability derivative module. The interrelationship of ZONAIR with other engineering software systems such as the pre-processor, structural finite element method (FEM), Computational Fluid

Dynamic (CFD) method, six degree-of-freedom (6 d.o.f.) and critical loads identification is depicted as follows.

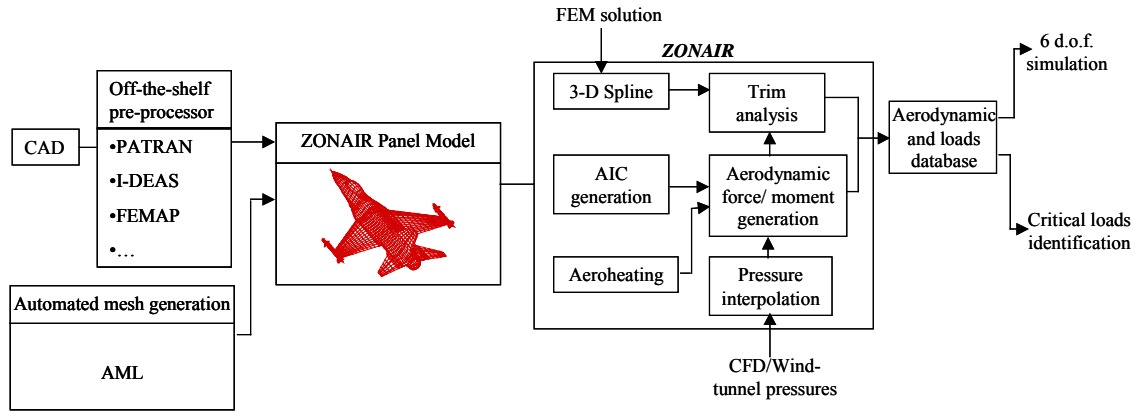


Fig 2 ZONAIR and It's Interfacing Capacity with Other FEM Software

ZONAIR has been under continuous development by ZONA throughout the last decade. ZONAIR's current version has proven capability accounting for multi-body interference, ground interference, wave reflection and store-separation, aerodynamics in hypersonic/supersonic as well as subsonic flow domains (Table 1). By comparison, ZONAIR is clearly the best choice as an expedient and versatile aerodynamic methodology. In what follows, we present the ZSTREAM development along with the hypersonic aerodynamics/aerothermodynamics applications based on ZONAIR whose results are compared with that of CFL3D [12]. These include:

- CKEM(Compact Kinetic Energy Missile) at  $M = 6.0$ ,  $\alpha = \pm 2^\circ$
- $15^\circ$  Blunt Cone at  $M = 10.6$  and  $\alpha = 5^\circ$
- X-34 at  $M = 6.0$ ,  $\alpha = 9^\circ$  and altitude = 183 Kft

Finally, a TPS sizing example employing heat rate input provided by ZONAIR + SHABP [13] from its coupled trajectory/aeroheating solution, is presented.

Table 1. Comparison of Various Aerodynamic Codes.

| Code                       | Method                      | Comp. Eff. (X-34) | Grid Gen. | Subsonic/Supersonic/Hypersonic | Multi Body Interf  | Ground Effect      | Aero-heating | Geo. High Fidelity | 6 DOF Store Sep. | Aeroload at FEM GRID |
|----------------------------|-----------------------------|-------------------|-----------|--------------------------------|--------------------|--------------------|--------------|--------------------|------------------|----------------------|
| CFL3D                      | Euler/NS                    | 30 hrs            | Needed    | All                            | Yes                | Yes                | Yes          | Yes                | No               | No                   |
| ZONAIR                     | Potential + Perturbed Euler | 20 min            | No        | All                            | Yes                | Yes                | Yes          | Yes                | Yes              | Yes                  |
| APAS                       | Potential + Empirical       | <10 min           | No        | Empirical in hyper-sonics      | Sub + Super-sonics | Sub + Super-sonics | Yes          | Low                | No               | No                   |
| PANAIR                     | Potential                   | 20 min            | No        | Sub + Supersonic               | Yes                | Yes                | No           | Yes                | No               | No                   |
| Component Build-up methods | Analytical + Empirical      | <<10 min          | No        | Yes                            | No                 | No                 | Yes          | Low                | No               | No                   |

### ***CKEM Hypersonic Aerodynamic Analysis using ZONAIR***

Under a recent Army/REDC support [4, 14], ZONA has further extended ZONAIR to treat body-fin configurations at Mach 6.0. To circumvent the superinclined panel problem (i.e., when the Mach line cuts into the body panel due to high Mach number), we introduce an equivalent Mach number transformation to recast the physical problem into a new coordinate, whereby the body undergoes a

compressibility stretch in the axial direction. A local pulsating body analogy has been established to account for shock/flow rotationally effects. ZONAIR is found to yield excellent trends following those of Exact Euler steady/unsteady solutions (Sims and Brong) in terms of static and dynamic stability derivatives throughout all Mach numbers from shock detachment to Mach 20. Expedient and accurate predictability in stability derivatives is one of the superior features of ZONAIR. A detailed theoretical formulation of ZONAIR is found in [4, 10].

Fig 3 shows the ZONAIR pressure distribution and aerodynamic force/moments along the CKEM body at M=6.0 for various bent-nose angles and angles of attack and compared with CFL3D results. In all cases, the ZONAIR results agree very well with those of CFL3D. Note that CFL3D requires over 2 hours of computer time for each bent-nose case whereas ZONAIR takes only 1 minute.

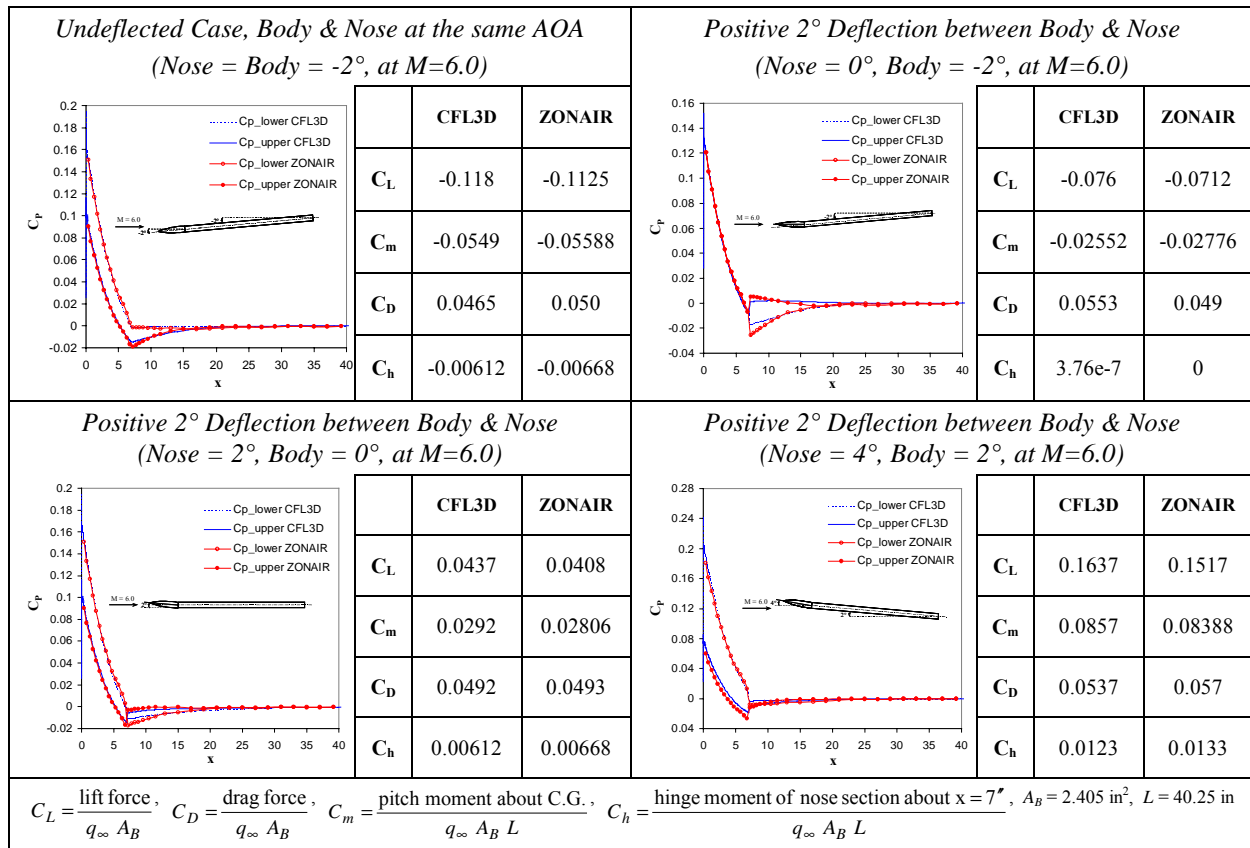


Fig 3 ZONAIR Pressure Distributions and Aerodynamic Force/Moments along the CKEM Body at M = 6.0 for Various Bent-Nose Angles and Angles of Attack

### ZSTREAM for Robust Streamline Computation

The development of ZSTREAM was prompted by the breakdown of QUADSTREAM in SHABP [13] at the stagnation points and its independency of freestream mach numbers. ZSTREAM is a finite element based streamline code, which is Mach number dependent and uniformly valid everywhere on the body surface. It is capable to define/plot high quality streamline solutions in the complete flow domain on the body surface, including the stagnation point, according to surface flow solutions given by a panel code (for example, ZONAIR) or a CFD code (For example, CFL3D). These streamline solutions of the CKEM body, the 15° blunt cone and X-34 are shown in Fig 4. ZSTREAM functionality is to provide streamlines input for Aeroheating/Heat-transfer programs such as SHABP for computations of the heat-transfer rate at the body surface.

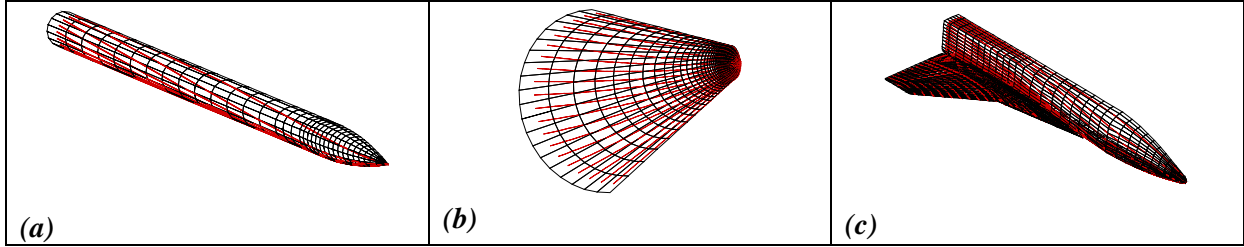


Fig 4 Streamline Results of (a) CKEM at  $M=6.0$  and  $\alpha=2^\circ$ ,  
 (b)  $15^\circ$  Blunt Cone at  $M=10.6$  and  $\alpha=5^\circ$ , (c) X-34 at  $M=6$  and  $\alpha=9^\circ$

**Aerothermodynamic Analysis by ZONAIR**

To validate the ZONAIR/ZSTREAM/SHABP procedure, we have performed the aeroheating analysis on three configurations, namely the CKEM body (Figs 5 and 6), a  $15^\circ$  blunt cone (Figs 7 and 8) and the simplified X-34 wing-body configuration (Figs 9 and 10). Note that the hypersonic boundary layer method in SHABP is developed based on the similarity solutions of compressible (laminar/turbulent) boundary layer methodology of Eckert/Boeing Rho-Mu, Spalding-Chi, and the White-Christoph methods [15]. The aeroheating results using the ZONAIR+ZSTREAM+boundary layer approach are validated with the CFL3D/Euler+LATCH [16] results on all cases considered. Good correlations on the inviscid  $C_p$ , heat transfer rates and surface temperature distributions can be seen from Figs 5-10.

It should be noted that the streamline computation procedure of LATCH is based on an integral method that contains a singularity at the stagnation point. This singularity prohibits the graphic capability of LATCH in the neighborhood of the nose, hence the cut out (Figs 6a, 8a). By contrast, ZONAIR is free from such singularity prohibition because of its finite element-based streamline procedure of ZSTREAM.

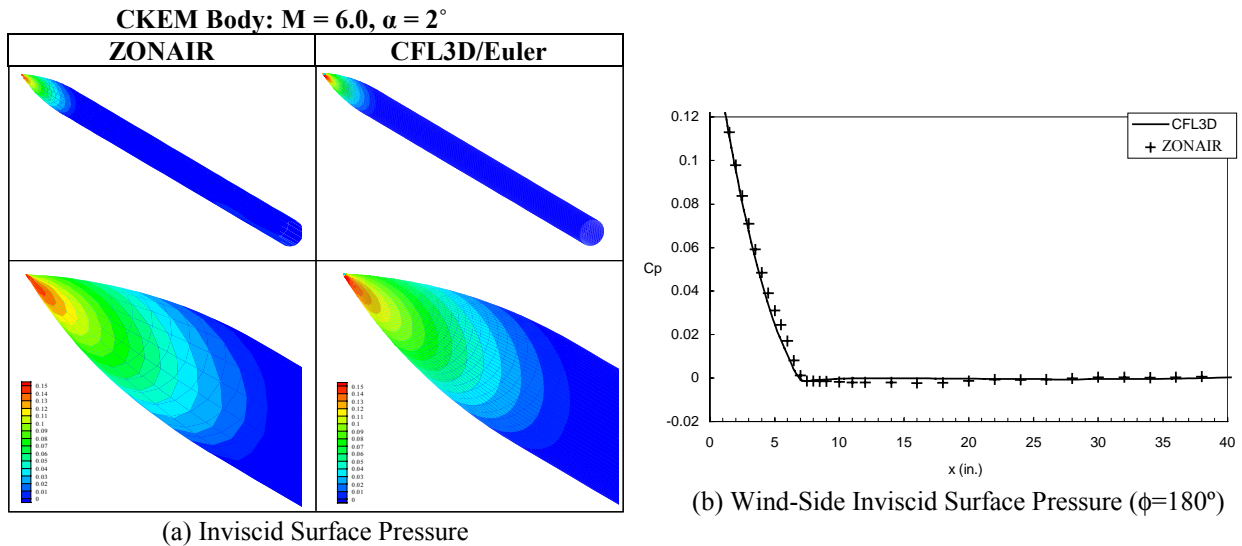
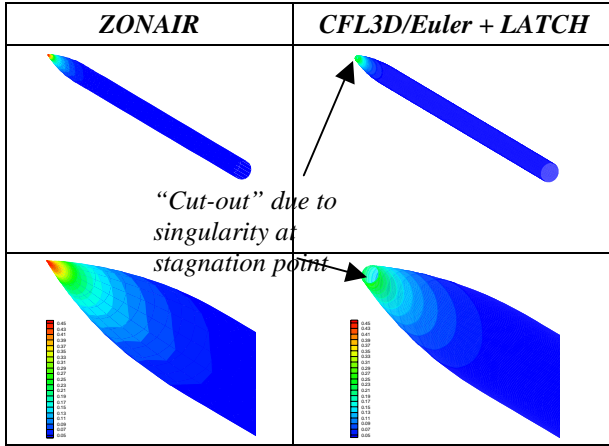
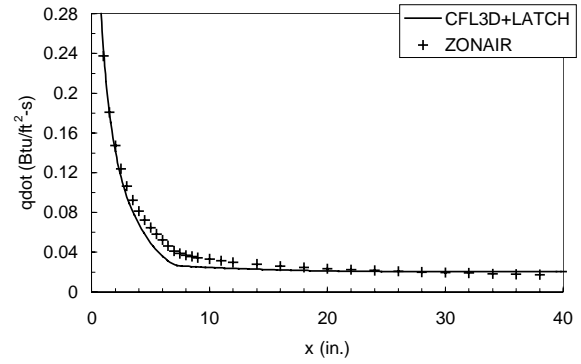


Fig 5 Inviscid Surface Pressure on CKEM at  $M_\infty=6.0, \alpha=2^\circ, p_\infty=2.66 \text{ lb/ft}^2, T_\infty=89.971^\circ\text{R}, T_w=540^\circ\text{R}$



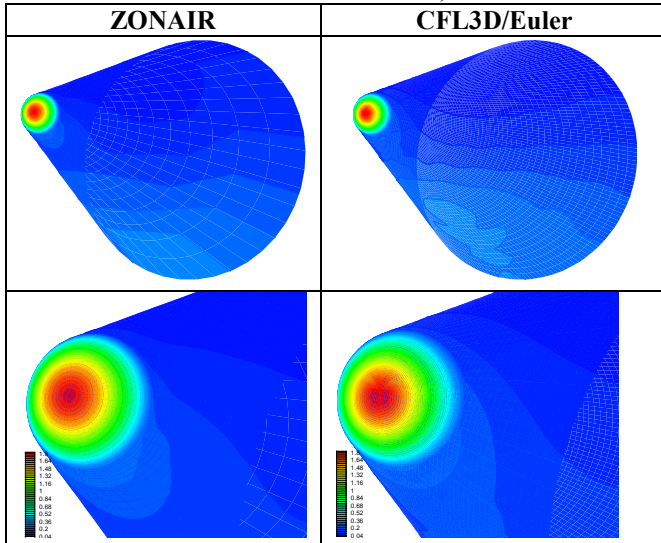
(a) Laminar Heat Transfer Rates (Btu/ft<sup>2</sup>-s)



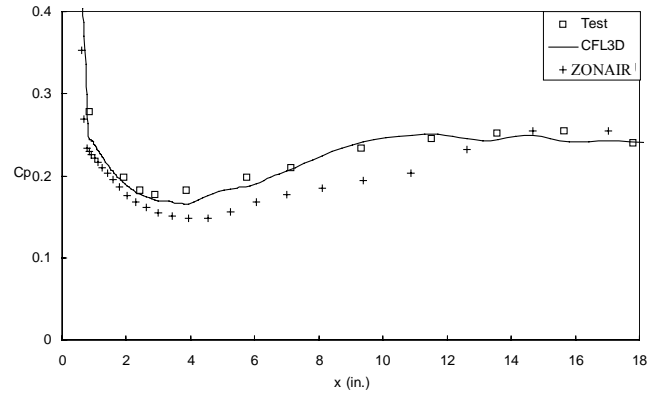
(b) Wind-Side Laminar Heat Transfer Rates ( $\phi=180^\circ$ )

Fig 6. Laminar Heat Transfer Rates on CKEM at  $M_\infty=6$ ,  $\alpha=2^\circ$ ,  $p_\infty=2.66$  lb/ft<sup>2</sup>,  $T_\infty=89.971^\circ\text{R}$ ,  $T_w=540^\circ\text{R}$ .

**15° Blunt Cone:  $M = 10.6$ ,  $\alpha = 5^\circ$**

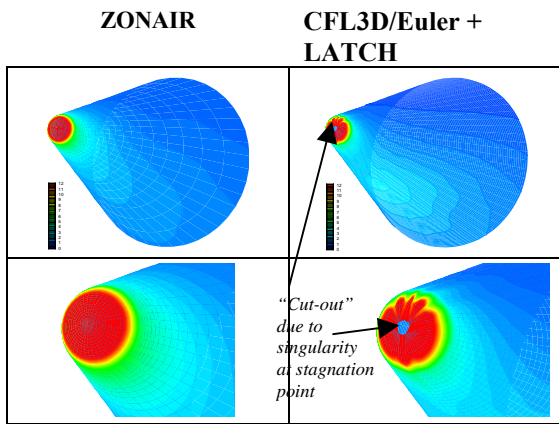


(a) Inviscid Surface Pressure

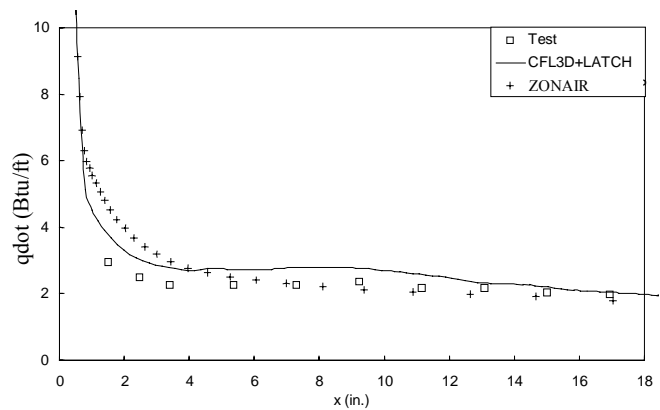


(b) Wind-Side Inviscid Surface Pressure ( $\phi=180^\circ$ )

Fig 7. Inviscid Surface Pressure on a 15° Blunt Cone at  $M_\infty=10.6$ ,  $\alpha=5^\circ$ ,  $p_\infty=2.66$  lb/ft<sup>2</sup>,  $T_\infty=89.971^\circ\text{R}$ ,  $T_w=540^\circ\text{R}$



(a) Laminar Heat Transfer Rates (Btu/ft<sup>2</sup>-s)



(b) Wind-Side Laminar Heat Transfer Rates ( $\phi=180^\circ$ )

Fig 8. Laminar Heat Transfer Rates (Btu/ft<sup>2</sup>-s) on 5° Blunt Cone at  $M_\infty=10.6$ ,  $\alpha=5^\circ$ ,  $p_\infty=2.66$  lb/ft<sup>2</sup>,  $T_\infty=89.971^\circ\text{R}$ ,  $T_w=540^\circ\text{R}$ .

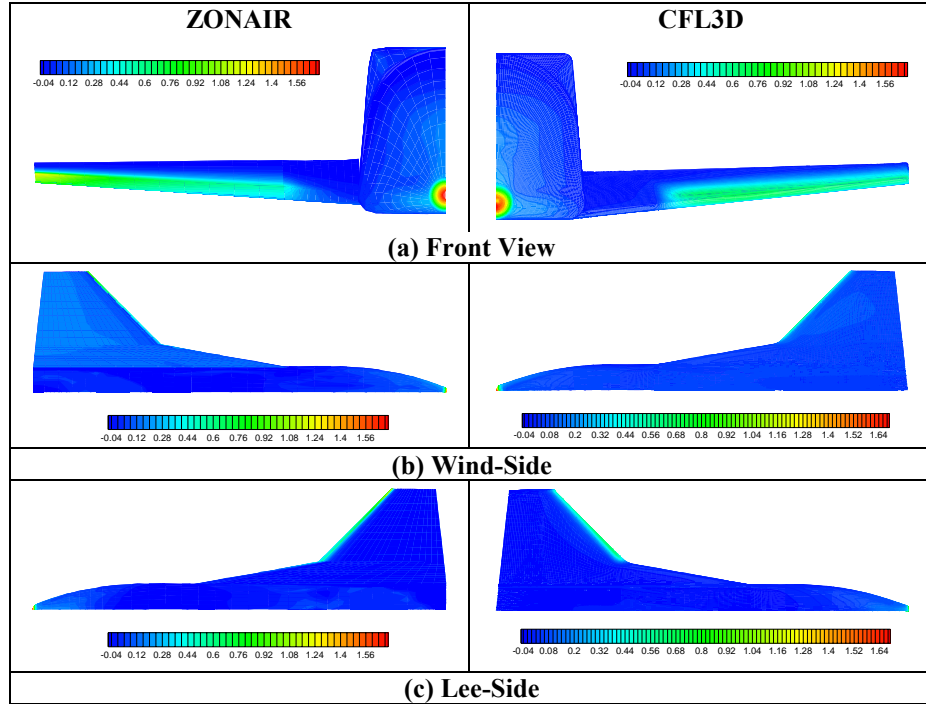


Fig 9. Inviscid Surface Pressure Distributions on the X-34 at  $M_\infty=6$ ,  $\alpha=9^\circ$ ;  
 (a) Front View, (b) Wind-Side, and (c) Lee-Side.

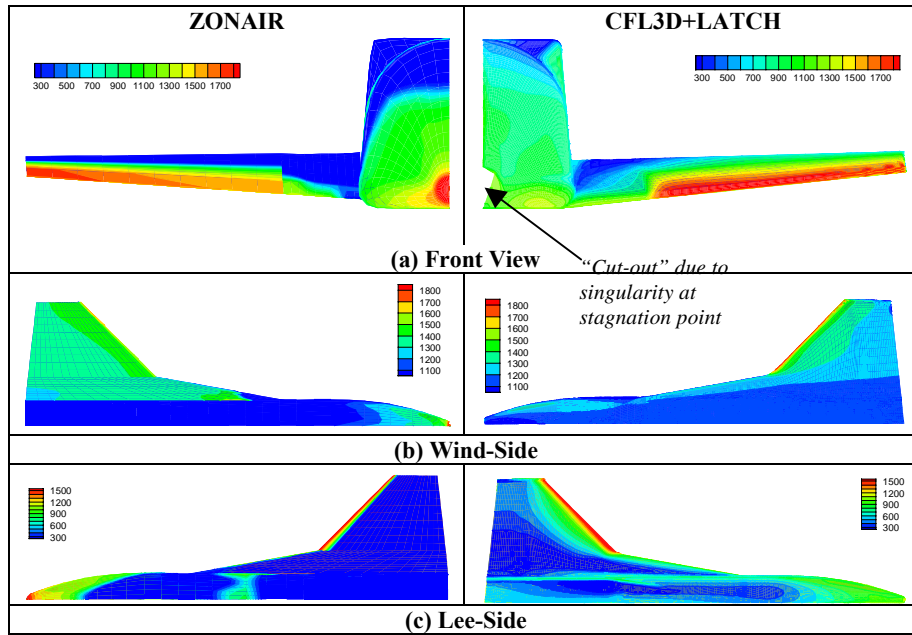


Fig 10. Turbulent Surface Temperatures ( $^\circ\text{F}$ ) on the X-34 at  $M_\infty=6$ ,  $\alpha=9^\circ$ ,  
 Alt.=183 Kft; (a) Front View, (b) Wind-Side, and (c) Lee-Side.

### Trajectory Analysis

The main function of the trajectory analysis is to obtain an optimal trajectory that minimizes the fuel while satisfying other constraints such as Mach number needed for specific engine usage, final velocities, altitudes, launch angle, etc.

Here, ZONAIR + SHABP is used to compute the heat rate at the stagnation point of the X-34 according to two assigned trajectories (X1004601 and X1004701). Good correlation is found between the present ZONAIR + SHABP method and MINIVER [11] (Fig 11).

ZONAIR + SHABP only requires the trajectory inputs to be submitted once, then it outputs the pressure ( $C_p$ , not shown) and the heat-rate ( $\dot{q}$ ) solutions. For 14 time steps along a stretch of 800 seconds of the flying time, it requires less than 10 minutes of computing time. By contrast, MINIVER requires manual input for each point of interest; i.e., each output  $\dot{q}$  curve requires approximately 5 to 10 minutes.

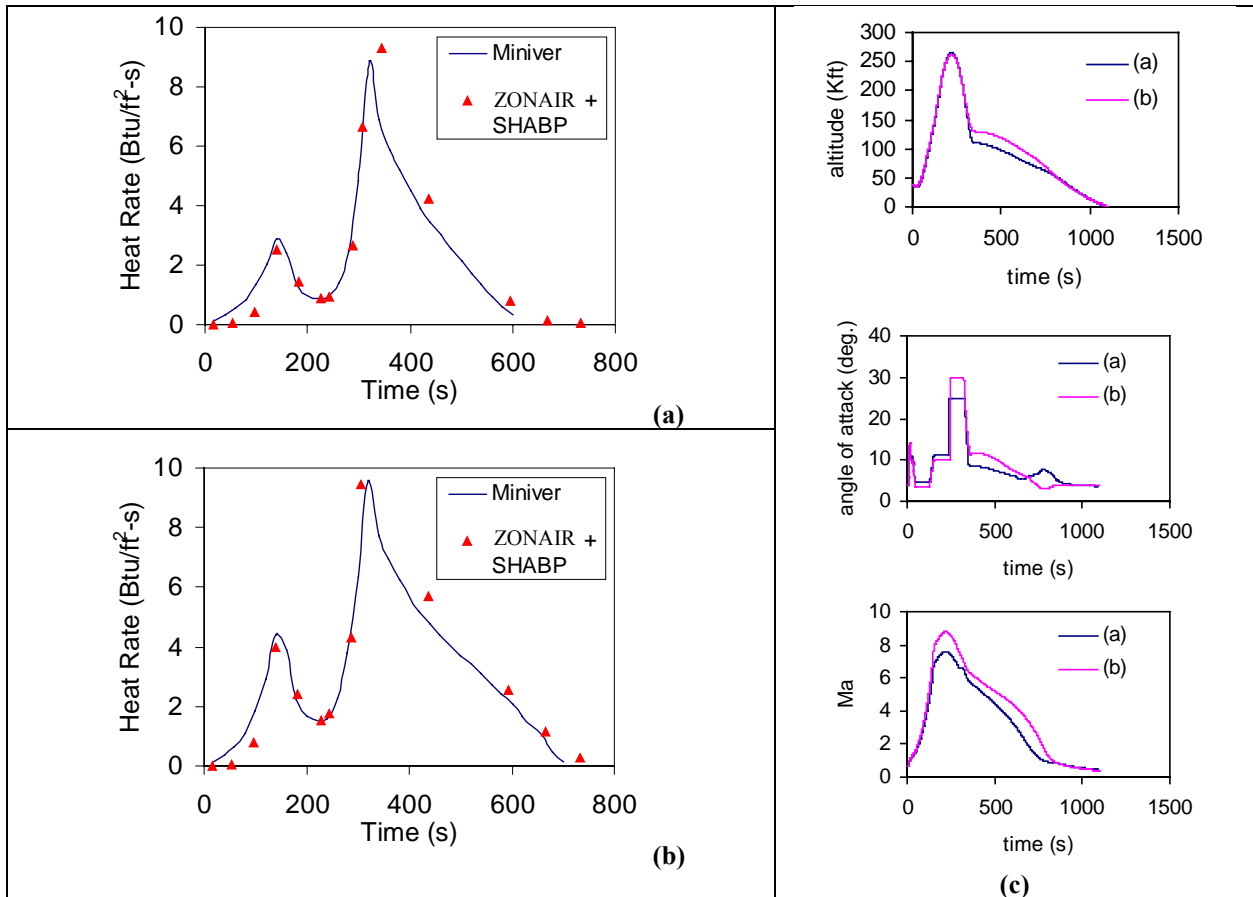


Fig 11. Heat Rate Comparison at Stagnation Point  
(a) X1004601, (b) X1004701, (c) Trajectory and flight condition history.

### TPS Sizing and Optimization

#### The TPS sizing procedure

The TPS sizing objective is to develop a procedure to minimize the TPS weight while satisfying the thermal protection requirement and the load-carrying requirement of the combined RLV/TPS structure. The developed TPS sizing procedure can be demonstrated by a constructed prototypical TPS/AFRSI (Advanced Flexible Reusable Surface Insulation) model [17]. (Fig 12)

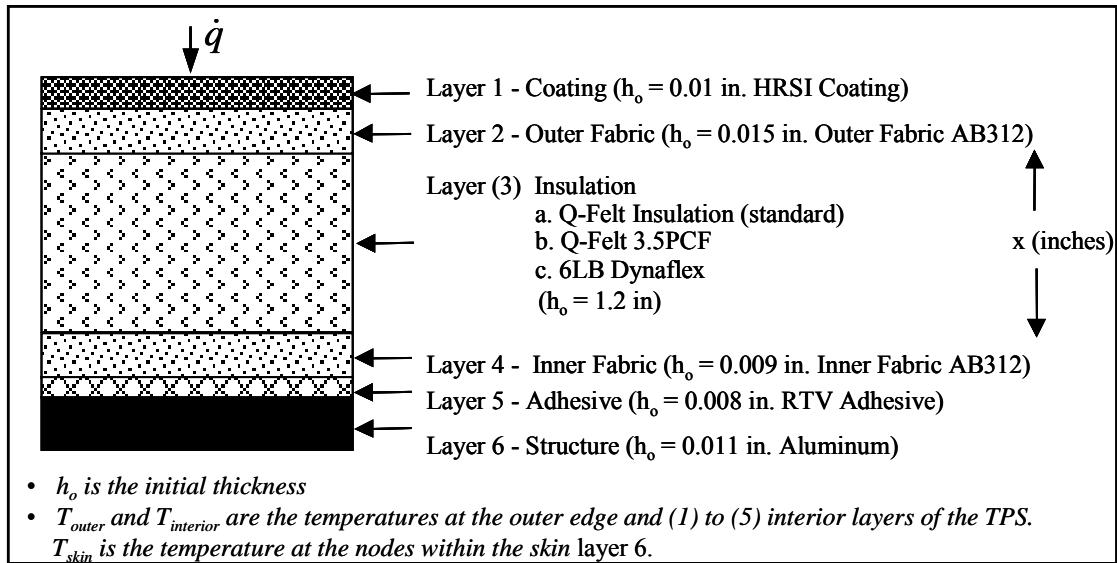


Fig 12. Description of the model TPS system (AFRSI from NASA TM 2000-210289 [17]).

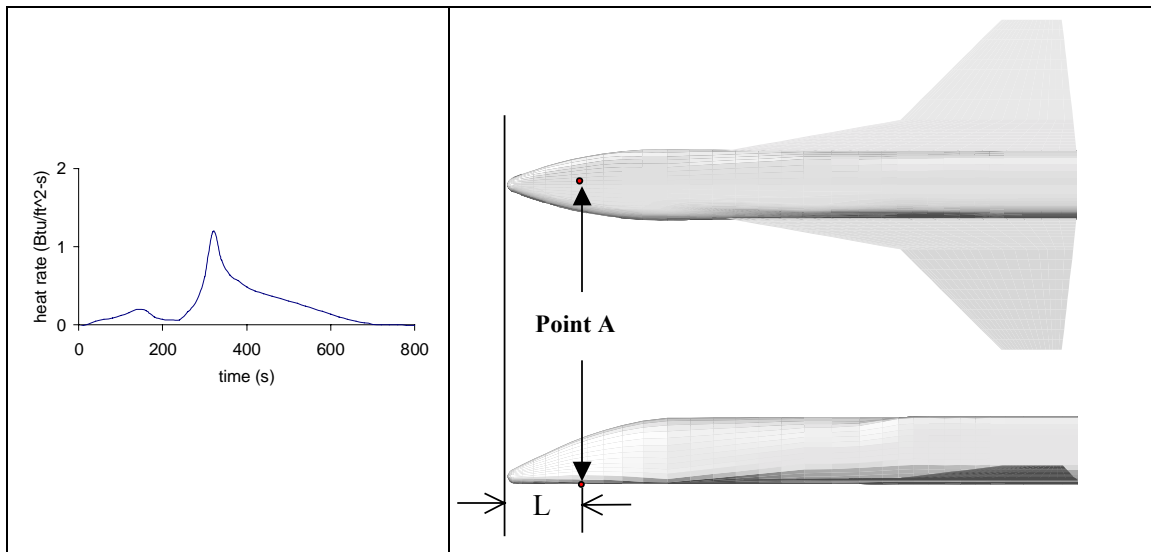


Fig 13. Location and Heat Flux History to Evaluate TPS Size on Windward Side of X-34 Centerline (bottom view and side view,  $L=50$  in.) Heat Flux is Based on Trajectory X1004601.

With this model, the objective becomes one to minimize the total weight of a TPS system as such. The inequality constraints are the maximum allowable operating temperature of each layer (characterized by the layer material) including that of the skin layer (Fig 12), whereas the thickness of each layer is the design variable. A typical TPS element, as an “elementary TPS system” is selected on the windward centerline of X-34 (Fig 13). The model input is the heat rate,  $\dot{q}$ , which is currently provided by ZONAIR+SHABP through the trajectory aerothermodynamic prediction (Fig 14). Maximum temperatures in each layer, layer thickness and the total minimum TPS weight are resulting outputs, obtained by applying the following optimization procedure to MINIVER/EXITS (Table 2). The developed code is called MINIVER/OPT.

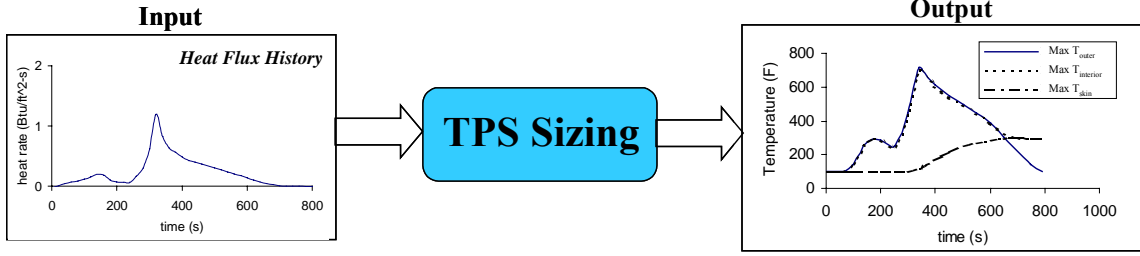


Fig 14 Input/Output of TPS Sizing

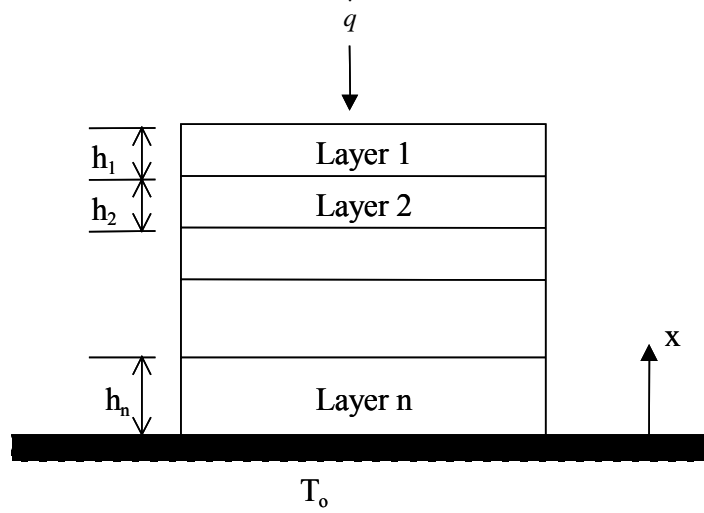


Fig 15 Typical TPS sizing problem

Fig 15 depicts a typical TPS design problem, which consists of  $n$  layers of different TPS materials. This design process can be automated by formulating an optimization problem statement as follows

$$\text{Minimize : } W = \sum_{i=1}^n \rho_i h_i$$

$$\text{Subject to : } T_i < T_{oi}, i = 1, 2 \dots n \quad (1)$$

$$\text{Design variable : } h_{\max i} \geq h_i, i = 1, 2 \dots n$$

where  $W$  is the total weight of the TPS system to be minimized,

$\rho_i$  is the density of the  $i$ th layer,

$T_i$  is the temperature in the  $i$ th layer,

$T_{oi}$  is the maximum operation temperature of  $i$ th layer's material,

$h_i$  is the thickness of the  $i$ th layer,

and  $h_{\max i}$  is the side constraint of the  $i$ th layer.

This optimization problem can be solved by linking a TPS analysis code such as MINIVER/EXITS [11] module with an optimization driver like the usable/feasible direction method imbedded in ASTROS [5]. One of the essential elements in the usable/feasible direction method is the sensitivity of the temperature time history of each layer with respect to the design variable  $h_i$ .

Many techniques, such as Finite Difference Method (FDM), Automatic Differentiation (ADIFOR), Symbolic Differentiation, the Complex Variable Differentiation (CVD) technique, can be adopted and applied to the MINIVER/EXITS module to provide sensitivity. Among them, the CVD technique is

selected because by comparison it is a “numerically-exact” method and requires the least programming effort.

The Complex Variable Differentiation (CVD) technique was first originated by Lyness and Moler [18]. In the complex variable approach, the variable  $x$  of a real function  $f(x)$  is replaced by a complex one,  $x + i\Delta h$ . For small  $\Delta h$ ,  $f(x + i\Delta h)$  can be expanded into a Taylor’s series as follows:

$$f(x + i\Delta h) = f(x) + i\Delta h \frac{df}{dx} - \frac{\Delta h^2}{2} \frac{d^2 f}{dx^2} - i \frac{\Delta h^3}{6} \frac{d^3 f}{dx^3} + \frac{\Delta h^4}{24} \frac{d^4 f}{dx^4} \dots \quad (2)$$

The first and second derivatives of the above equation can be expressed as:

$$\frac{df}{dx} = \frac{\text{Im}[f(x + i\Delta h)]}{\Delta h} + O(\Delta h^2) \quad (3)$$

$$\frac{d^2 f}{dx^2} = \frac{2[f(x) - \text{Re}(f(x + i\Delta h))]}{\Delta h^2} + O(\Delta h^2) \quad (4)$$

where the symbol “Im” and “Re” denote the imaginary and real parts, respectively. From Eqs. (3) and (4), it can be seen that the derivatives using the CV approach only require function evaluations. This feature is very attractive particularly when the function is sufficiently complicated, in which case to obtain an analytic derivative is cumbersome and error-prone. Unlike the finite difference method, where the accuracy of the derivative depends on the step-size, Eq. (3) shows that the first derivative does not involve differencing two functions followed by magnification of the subtraction error (because of the division by the step size  $\Delta h$ ). In fact, no cancellation errors exists for the first derivative in the CVD technique, thus the first derivative is step-size independent. Note that the second derivative in Eq. (4) is prone to cancellation errors (because of the subtraction of two close numbers), but is not used here.

Because CVD does not introduce cancellation (roundoff) error for the first derivative, the step-size  $\Delta h$  can be chosen as small as the machine zero, e.g.,  $\Delta h = 10^{-30}$ . Hence, the truncation error due to Taylor’s series of the order of  $\Delta h^2 = 10^{-60}$  that approaches to essentially a machine zero in a 32 bit computer. For first derivative, CVD does not seem to introduce any approximation in its numerical differentiation, rather it is a nearly “numerically-exact” differentiation technique.

To incorporate CVD into the MINIVER/EXTIS module (called MINIVER/OPT) for sensitivity is rather straightforward. One can simply declare all variables in the code as complex variable and introduce a small imaginary perturbation ( $i\Delta h = i \times 10^{-30}$ ) in the design variable  $h_i$ . Division of the imaginary part of the temperature time history in each layer by  $\Delta h$  yields the sensitivity.

To validate the accuracy of the sensitivity MINIVER/OPT, we select the constructed prototypical TPS system using an AFRSI (Advanced Flexible Reusable Surface Insulation) module, Fig. 12.

With the given heat/flux  $\dot{q}$  at point A (depicted in Fig 13) we focus on the temperature sensitivity of layer 6. The sensitivity  $\frac{\partial T_6}{\partial h_3}$ , which precisely corresponds to the temperature change at the aluminum structure due to the thickness perturbation of the Q-Felt insulation material (layer No. 3), computed by MINIVER/OPT is shown in Figure 16. The negative values of the sensitivity indicate the decrease of

temperature due to the increase of thickness; as expected. Comparing to the results of CVD, the relative error of the sensitivity computed by FDM with various step size is depicted in Fig 17. It can be seen that the error of FDM decreases while the step size decreasing. But with a very small step size ( $\Delta h = 10^{-8}$ ), the error increases, showing that the accuracy of FDM is step-size dependent.

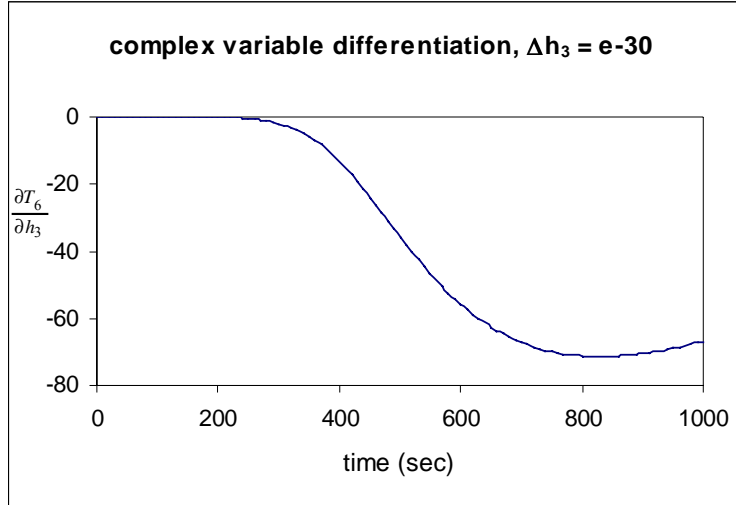


Fig 16 Sensitivity  $\partial T_6/\partial h_3$  by MINIVER/OPT in the entire history

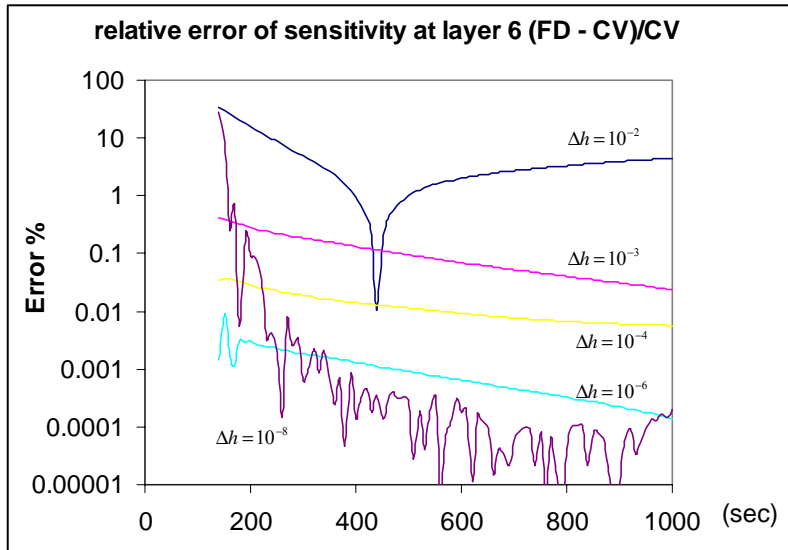
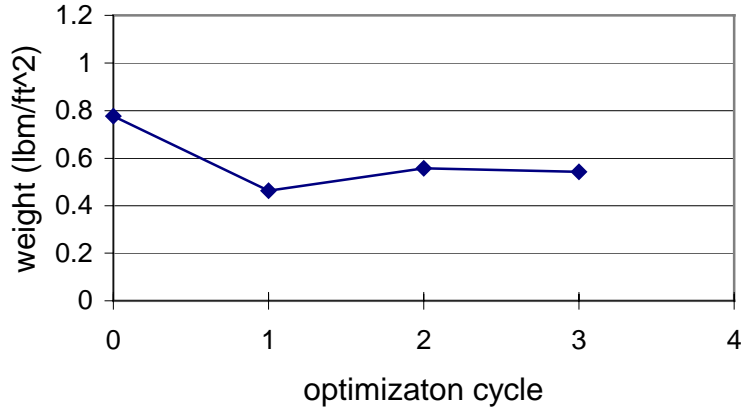
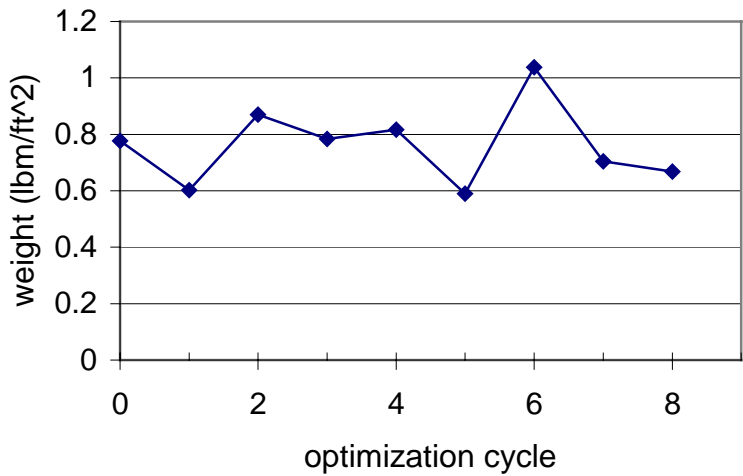


Fig 17 Relative error of FDM and CVD for sensitivity  $\partial T_6/\partial h_3$



(a) Case A with a given  $\dot{q}$  (in 263 Sec)



(b) Case B with  $1.5x \dot{q}$  (in 396 Sec)

Figure 18 Weight variation of the modeled TPS System (AFRSI) during optimization

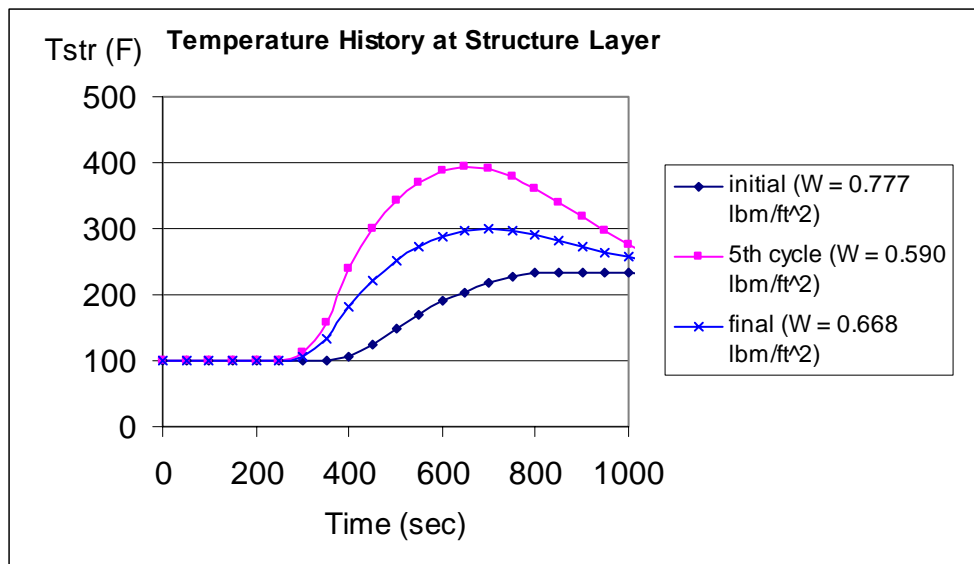


Fig 19 Case B Temperature history at the structure layer (Layer 6) during optimization process

Table 2 Case A Optimization Results

| Layer | Material and Temp limit (°F) | density (lbm/ft <sup>3</sup> ) | Specific heat (But/lbm° F) | Initial thickness (in) | T <sub>max</sub> in layer (°F) | Optimized thickness (in) |
|-------|------------------------------|--------------------------------|----------------------------|------------------------|--------------------------------|--------------------------|
| 1     | HRSI Coating 2300            | 104                            | 0.20                       | 0.01                   | 705.2                          | 0.0072                   |
| 2     | AB312 Fabric 2024            | 61.5                           | 0.166                      | 0.015                  | 704.9                          | 0.0072                   |
| 3     | Q-Felt 1800                  | 3.5                            | 0.1875                     | 1.2                    | 701.6                          | 0.66849                  |
| 4     | AB312 Fabric 2024            | 61.5                           | 0.166                      | 0.009                  | 300.0                          | 0.0072                   |
| 5     | RTV-560 550                  | 88                             | 0.285                      | 0.008                  | 300.0                          | 0.0072                   |
| 6     | Aluminum 300                 | 173                            | 0.22                       | 0.011                  | 300.0                          | 0.011                    |

- Layer Thickness: upper bound 1.0”, lower bound 0.0072”
- Given Input heat flux  $\dot{q}$ , see Fig 13
- Optimized Weights  $W_{\text{initial}} = 0.777 \text{ lbm/ft}^2$ ,  $W_{\text{final}} = 0.543 \text{ lbm/ft}^2$

Shown in Table 2 is the optimization results of the AFRSI TPS system depicted in Figures 12 and 13 (Case A). In this optimization problem, the thickness of first five layers are defined as design variables with initial thickness and maximum operational temperature shown in Table 2. The upper bound and lower bound of these five design variables are assumed to be 1.0” and 0.0072”, respectively. The thickness of aluminum layer (layer 6) remains unchanged because it represents the load-carry structure and is not a part of the TPS system. It can be seen that all design variables reach the lower bound (0.0072”) except the Q-Felt layer. This is expected because the Q-Felt layer has the lowest density and thermal conductivity that provide the highest thermal insulation capability with least structural weight.

Table 3 Case B Optimization Results

| Layer | Material and Temp limit (°F) | density (lbm/ft <sup>3</sup> ) | Specific heat (But/lbm° F) | Initial thickness (in) | T <sub>max</sub> in layer (°F) | Optimized thickness (in) |
|-------|------------------------------|--------------------------------|----------------------------|------------------------|--------------------------------|--------------------------|
| 1     | HRSI Coating 2300            | 104                            | 0.20                       | 0.01                   | 814.5                          | 0.0072                   |
| 2     | AB312 Fabric 2024            | 61.5                           | 0.166                      | 0.015                  | 814.3                          | 0.0072                   |
| 3     | Q-Felt 1800                  | 3.5                            | 0.1875                     | 1.2                    | 810.0                          | 0.6000                   |
| 4     | AB312 Fabric 2024            | 61.5                           | 0.166                      | 0.009                  | 300.0                          | 0.0072                   |
| 5     | RTV-560 550                  | 88                             | 0.285                      | 0.008                  | 300.0                          | 0.02705                  |
| 6     | Aluminum 300                 | 173                            | 0.22                       | 0.011                  | 300.0                          | 0.011                    |

- Layer Thickness: upper bound 0.6”, lower bound 0.0072”
- Given Input heat flux  $1.5\dot{q}$ , see Fig 13
- Optimized Weights  $W_{\text{initial}} = 0.777 \text{ lbm/ft}^2$ ,  $W_{\text{final}} = 0.668 \text{ lbm/ft}^2$

Table 3 presents the optimization results of the same AFRSI TPS system but with a magnified heat flux (by a factor of 1.5) and a reduced upper bound in design thickness (Case B). The optimized result is that the thickness of the Q-Felt layer reaches the upper bound and that of the RTV-560 layer become 0.02705” while the thickness of other layers remain at the lower bound. This indicates that because of the higher heat flux input, the Q-Felt layer with the upper bound thickness alone is not sufficient to satisfy the temperature constraints at all layers. Other than the Q-Felt layer, the next best thermal protection material is the RTV-560 layer because of its highest value of specific heat ( $c_p$ ). Although, the RTV-560 layer has a high density  $\rho$  which may not be structurally efficient, however, its higher  $\rho c_p$  value can offer a good thermal protection capability. Indeed, MINIVER/OPT can detect this capability and thereby increase the thickness of the RTV-560 layer from the lower bound to 0.02705”.

Figures 18 presents the weight variance versus design cycles during the optimization process. Note that case A the nominal heat-flux achieves optimized weight with 3 cycles in 4.5 minutes; whereas case B (with 1.5 times heat-flux) takes 8 design cycles in 6.5 minutes.

Figure 19 presents the time history of the temperature of Case B of the aluminum layer during its eight optimization design cycles. With the maximum operational temperature being 300°F of the aluminum as one of the design constraints, it can be seen that the initial thickness is over-designed because its maximum temperature is only approximately 230°F. Meanwhile, an intermediate design offers a least weight but its maximum temperature (400°F) violates the constraint. The maximum temperature of the final design is exactly 300°F, indicating that it is an optimum design.

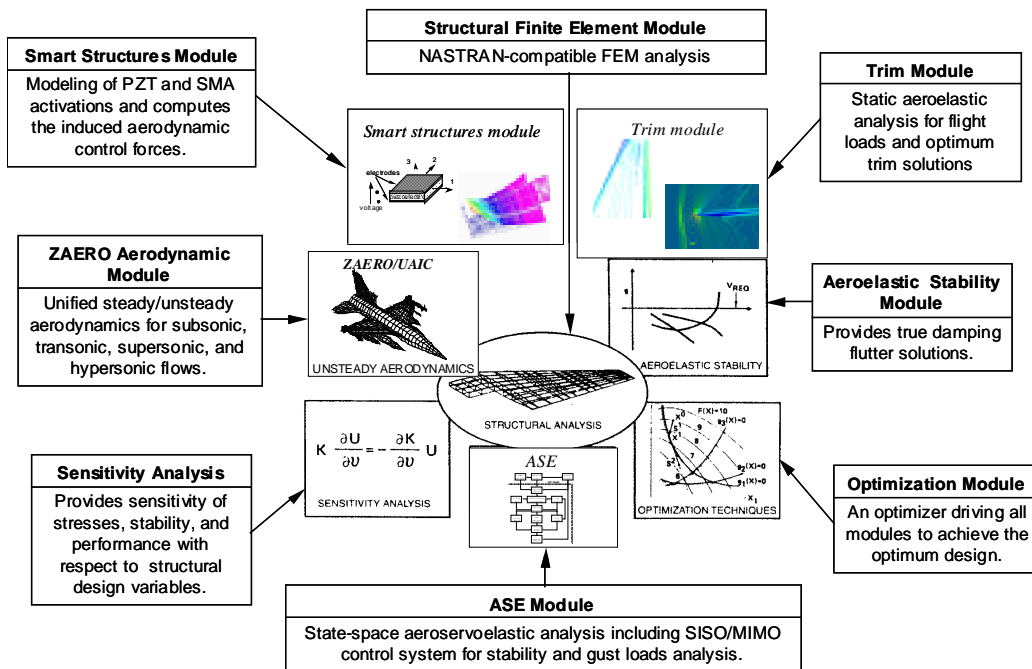


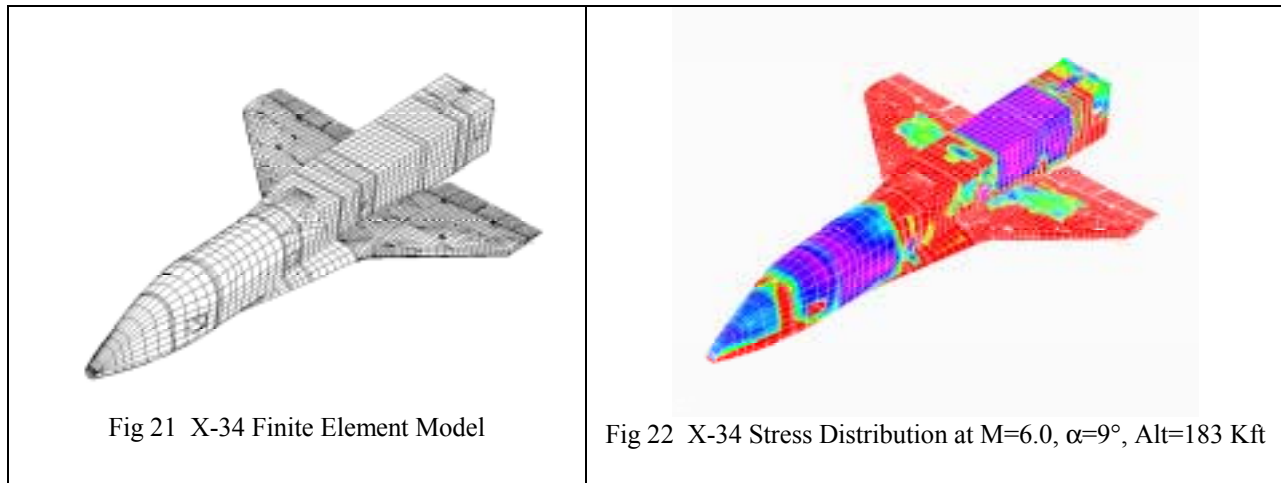
Fig 20 Engineering Modules in ASTROS\*

### TRIM Analysis using ASTROS\* and ZONAIR

ASTROS\* is an enhanced version of ASTROS (Automated Structural Optimization System [5]), an internationally acclaimed MDO software developed by Northrop Grumman Corporation for the Air Force. Under a two-year contractual support by AFRL, ZONA has further enhanced ASTROS by seamlessly integrating several engineering modules into ASTROS [19, 20]. Fig 20 depicts all the essential modules of ASTROS\*, including a unified aerodynamic module (ZAERO), a NASTRAN-based

structural finite element module, a smart structure module, a trim module, an aeroelastic stability module, an aeroservoelastic module, a sensitivity analysis module, and an optimization module.

The trim analysis for the flexible X-34 is performed using ASTROS\* in conjunction with ZONAIR to account for the static aeroelastic effect of the vehicle. The outcomes of the trim analysis are the control surface deflection angles, load factors, etc. as well as the stress distribution in the structures. Fig 21 depicts an ASTROS\* finite element model of the X-34 that includes the modeling of the TPS mass and the material property degradations on the load carrying structure due to aeroheating effects as computed by ZONAIR. The ASTROS\* trim analysis shows that in order to trim the X-34 at  $M = 6.0$ ,  $\alpha = 9^\circ$  and altitude = 183 Kft, the required trailing edge flap angle is  $2.05^\circ$  degrees and a load factor of 0.97-g for a total weight of 16,000 lbs. At this condition, the aerodynamic loads computed at the ZONAIR panels are then mapped to the FEM grid using the 3D spline module; allowing a subsequent stress analysis of the structures. Such a stress distribution is shown in Fig 22.



### ***Temperature Mapping for Aerothermoelastic Analysis***

- Temperature and Aeroloads Mapping from Aerodynamic to Structural Grids

For the present aerothermoelastic analysis, two types of data mapping between the aerodynamic grid (the aerodynamic panels) and the structural finite element (FEM) grid are required. The first type is the mapping of the aerodynamic forces from the aerodynamic grid to the structural grid as well as the displacement from the FRM grid back to the aerodynamic grid. This type of data mapping procedure has been fully developed in ASTROS\*, and has been applied to the previous ZONAIR/TRIM analysis for the force mapping. The second type of mapping is one that transfers the temperature distribution on the skin of RLV to that on the outmost structural surface. Note that this is strictly a grid system mapping for temperature transferal whereas no heat transfer is assumed to take place. In terms of finite element context, this amounts to the mapping of the temperatures (of the TPS skin layer) from the ZONAIR surface grid to the outmost FEM grid.

Since, FEM elements/grids are filled within and extended to the surface of the RLV it is required to identify the outmost FEM surface compatible with the ZONAIR surface for temperature mapping. As these two surfaces are likely to be misaligned, then a projection scheme is required to perform the temperature mapping “outward” or “inward” from the ZONAIR surface grids.

The second type mapping requirement is the temperature mapping from the aerodynamic grid to the FEM surface grid. There are two technical challenges involved in the development of such a mapping procedure:

- (1) Because the FEM model contains elements/grids on the surface skin as well as the internal structures, it is required to identify those only on the surface skin for temperature mapping.
- (2) Because the wet surface skin defined by the ZONAIR mesh and FEM surface mesh may have discrepancy, the temperature mapping requires a projection procedure that can either project “outward” or “inward” from the ZONAIR panels.

- Temperature Mapping Procedure

A finite-element procedure has been developed for temperature mapping that assumes the coordinates and temperatures at any point on the ZONAIR model can be determined by the nodal values of the ZONAIR panels through the shape functions expressed as

$$X = \sum_{\alpha} N_{\alpha}(\xi, \eta) X^{\alpha} \quad (5)$$

where  $X$  is the coordinates or temperatures at any given point

$N_{\alpha}(\xi, \eta)$  is the shape functions and  $\xi, \eta$  are the intrinsic coordinate of the shape function

$\alpha$  is the number of nodes of a ZONAIR panel, and

$X^{\alpha}$  is the coordinates or temperatures at ZONAIR nodes.

For a given structural FEM grid  $p$  as shown in Figure 23, the point  $q$  on the ZONAIR model that has the minimum distance to  $p$  can be found by solving

$$X - X^p = \lambda n \quad (6)$$

where  $X$  is the coordinates of point  $q$

$X^p$  is the coordinates of point  $p$

$n$  is the out-normal of vector of the ZONAIR panel, and

$\lambda$  is a multiplication factor to  $n$ .

A FEM grid  $p$  is a surface grid only if no FEM elements are located between the points  $p$  and  $q$ . This condition can be determined by solving the following equation

$$X - X^p = t(X^q - X^p) \quad (7)$$

Figure 24 shows a FEM element that is located between the points  $p$  and  $q$ . The point  $s$  on the element which intersects the vector  $X^q - X^p$  has the conditions such that  $-1 \leq \xi \leq 1$ ,  $-1 \leq \eta \leq 1$  and  $-1 \leq t \leq 1$ , where  $t$  is the position tracking parameter.

To validate the above procedure, we select the X-34 FEM model as the test case. Fig 25a depicts the X-34 FEM model that consists of surface skin elements as well as the elements modeling the internal structures. The resulting surface grid and elements are shown in Figure 25b where the removal of the internal structures can be clearly seen.

Once the FEM grid is identified as a structure grid, then its temperature is assumed to be the same as that at the closest ZONAIR surface point. It should be noted that the temperature at any ZONAIR surface points can be calculated using the shape function shown below

$$T = \sum_{\alpha} N_{\alpha}(\xi, \eta) T^{\alpha} \quad (8)$$

where  $T^\alpha$  is the temperature at the ZONAIR nodal points.

Shown in Figure 26a and 26b is a temperature distribution computed on the X-34 ZONAIR model and the mapped temperature on the FEM surface grid/elements. Overall, the mapped temperature agrees well with the computed temperature, showing the accuracy of the developed temperature mapping methodology.

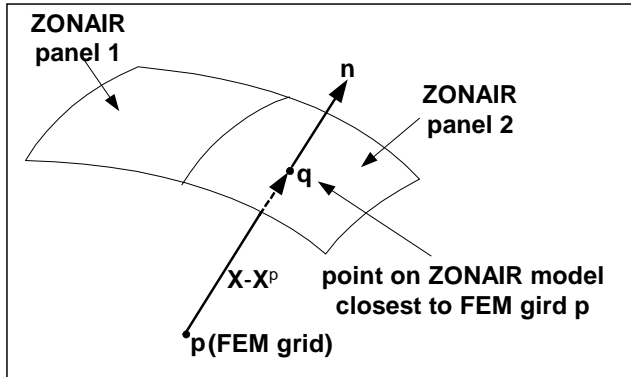


Fig 23 Minimum distance between the FEM grid p and a point on the ZONAIR model q

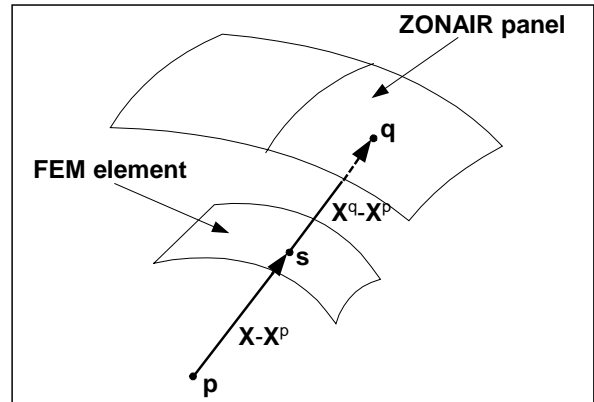
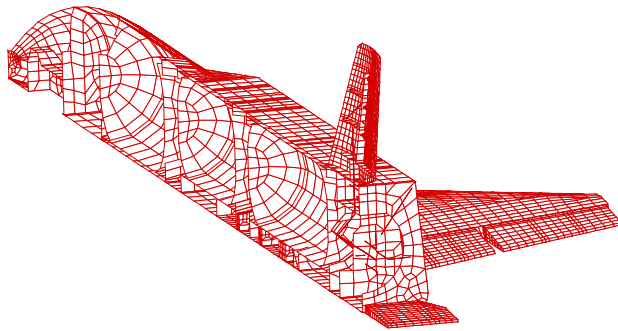
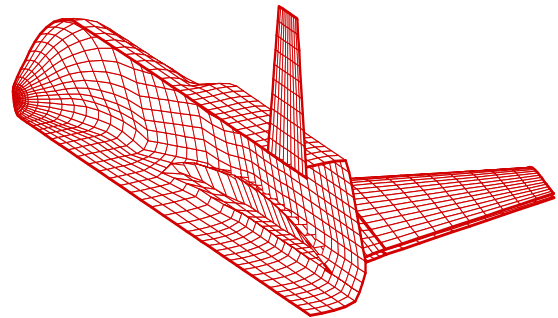


Fig 24 A FEM element located between point p and q

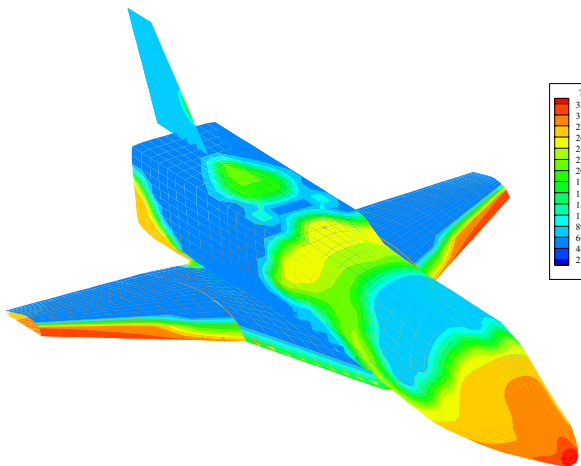


(a) X-34 full FEM model

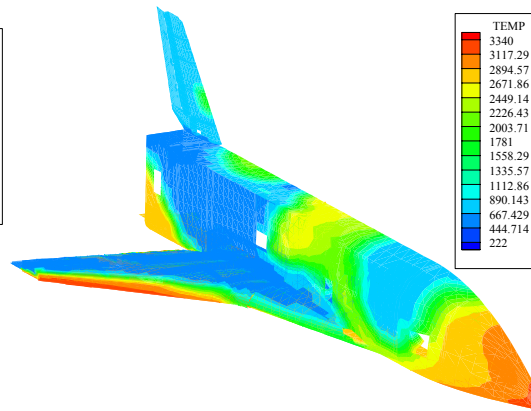


(b) X-34 surface grid/elements

Fig 25 Removal of the internal grid and elements on the X-34 FEM model



(a) Temperature distribution computed on ZONAIR model



(b) Mapped temperature on FEM surface elements/grids

Fig 26 Temperature mapping results on the X-34 FEM model

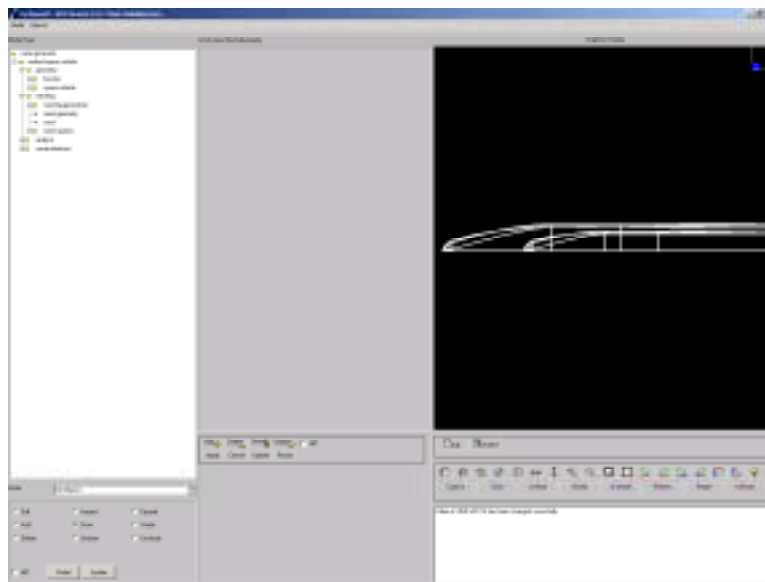
### ***Automated Mesh Generation using AML***

Present ZONAIR/ASTROS integration effort directs toward a fully user-oriented aerothermodynamic/aerothermoelastic tool for RLV/TPS design. To this end, their integration with design-oriented automated mesh generation software is desirable. Prior integration of AML (adaptive modeling language) with SHDV (supersonic hypersonic vehicle design) system has shown the former is a viable user-oriented mesh generator suitable for aerospace vehicle design. Its capability to generate and rapidly alter design configuration is controlled by a set of essential generic geometric parameters. In fact, AML could manage and automate the data transfer between various design and analyses tools. [6]

Specifically, AML can expediently generate FEM element meshes for NASTRAN as well as that for ASTROS, because both use the same bulk data input format. Adopted a unstructured finite-element type panel scheme, ZONAIR also shares a similar bulk data input format. Thus, applying AML to ZONAIR/ASTROS for mesh generation is a straightforward task. Our next step is to integrate ZONAIR/ASTROS and the other software in the aerothermodynamic/aerothermoelastic architecture (Figure 1) with AML into a feature-based design environment.

Presented here are some preliminary results generated by the coupling of AML with ZONAIR demonstrating a 2-body RMLV design process. Figure 27 shows various views of the 2-body RMLV design. Figure 28 shows the automated generation of ZONAIR Panels by AML. Figure 29 presents the pressure and Mach number distributions, showing effects of supersonic wave interference between 2-bodies.

## **Demo of Automated Panel Generation Using AML Reusable Military Launch Vehicle (RMLV)**

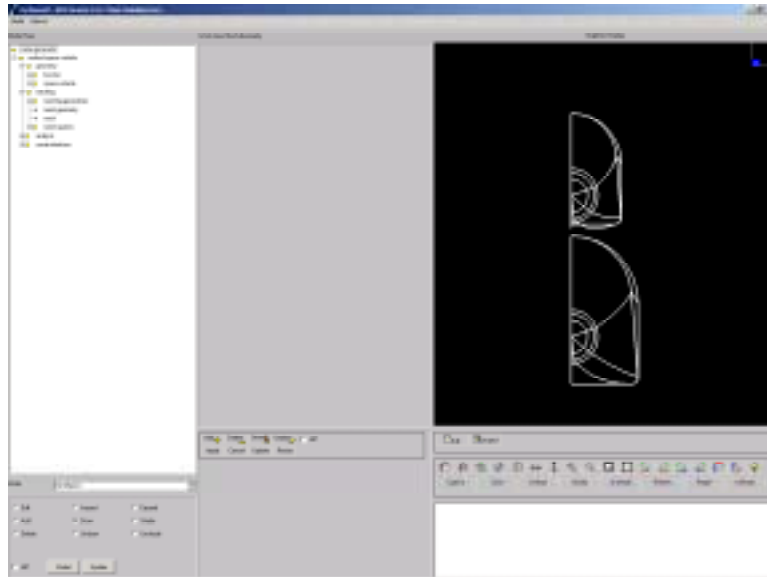


a. Top View

Fig 27 Demo of Automated Panel Generation of RMLV using AML

## Demo of Automated Panel Generation Using AML Reusable Military Launch Vehicle (RMLV)

---

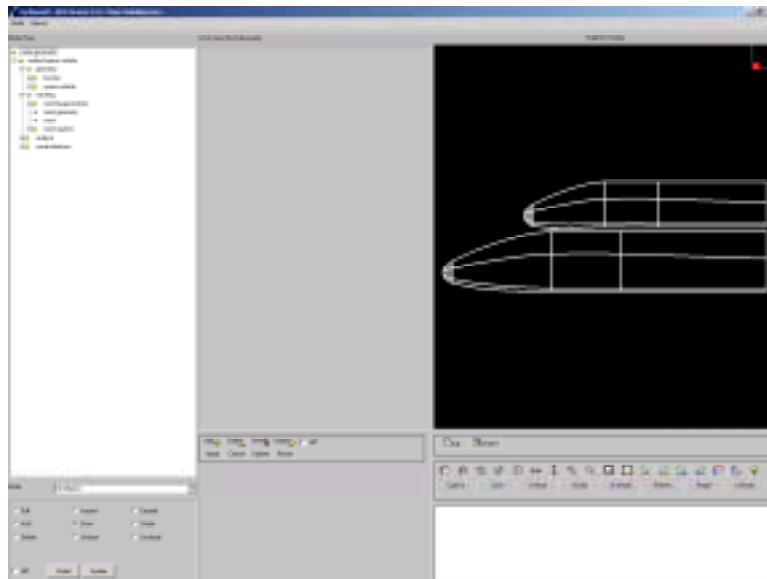


b. Front View

Fig 27 Demo of Automated Panel Generation of RMLV using AML

## Demo of Automated Panel Generation Using AML Reusable Military Launch Vehicle (RMLV)

---

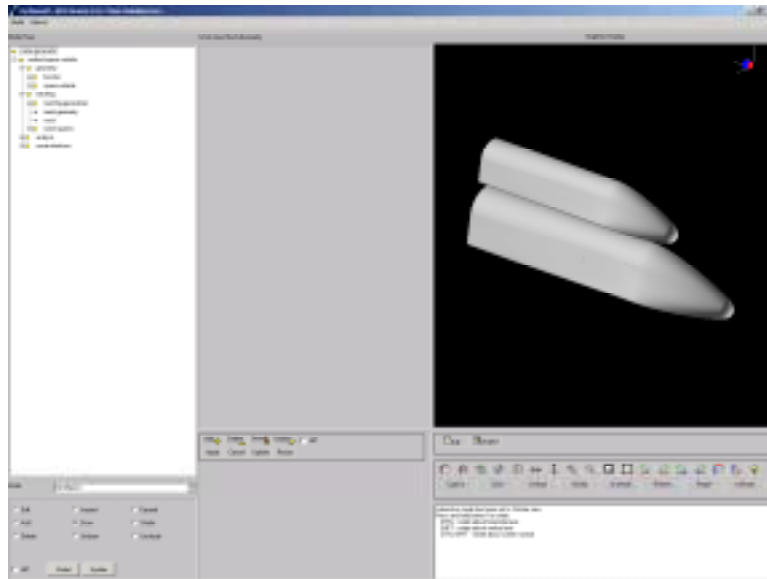


c. Side View

Fig 27 Demo of Automated Panel Generation of RMLV using AML

## Demo of Automated Panel Generation Using AML Reusable Military Launch Vehicle (RMLV)

---



d. 3D View

Fig 27 Demo of Automated Panel Generation of RMLV using AML

## Demo of Automated Panel Generation Using AML ZONAIR Panel Model of RMLV

---

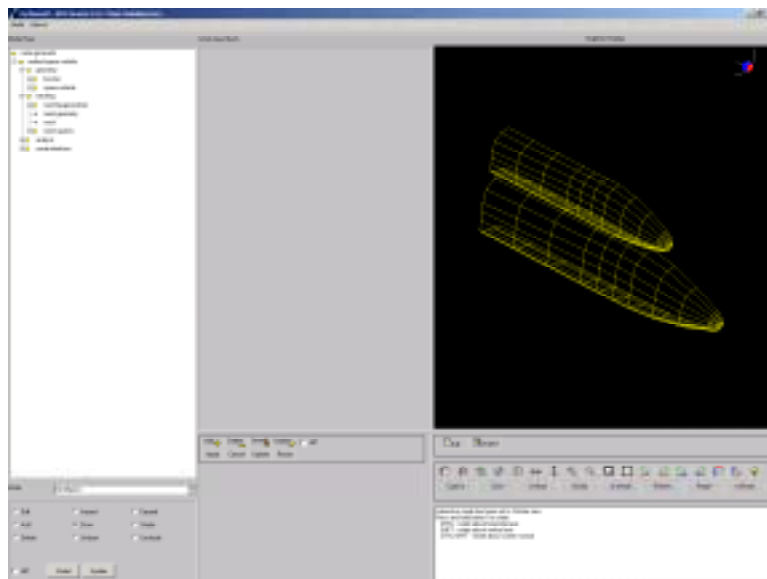
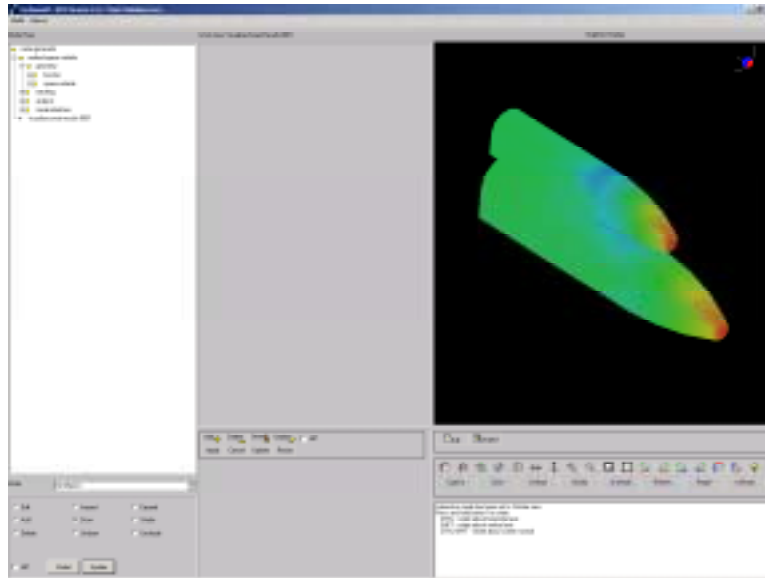


Fig 28 Demo of Automated Panel Generation of AML/ZONAIR

## Demo of Automated Panel Generation Using AML Pressure Distribution at $M = 1.2, \alpha = 0^\circ$

---

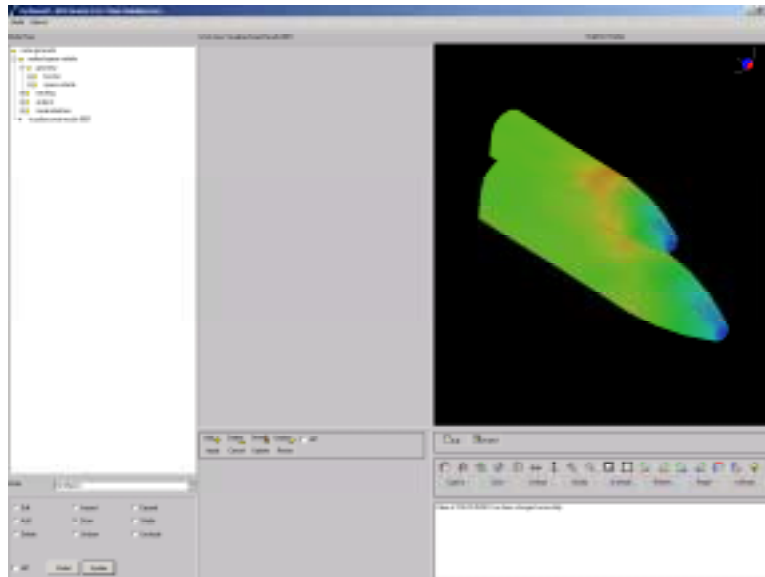


a.

Fig 29 Demo of Automated Panel Generation of AML/ZONAIR Aerodynamics

## Demo of Automated Panel Generation Using AML Mach Number Distribution at $M = 1.2, \alpha = 0^\circ$

---



b.

Fig 29 Demo of Automated Panel Generation of AML/ZONAIR Aerodynamics

### **Concluding Remarks**

ZONAIR is a *mid-level* computational method between the high level CFD method and lower level engineering methods. *ZSTREAM* was developed to replace the Newtonian-based streamline generator in SHABP in order to improve coupling solutions between the boundary layer option of SHABP and

ZONAIR. When interfaced with SHABP, ZONAIR is shown to be a viable hypersonic aerothermodynamic software for expedient RLV/TPS design and analysis. Feasibility studies of various configurations including CKEM body, blunt cones, and X-43 have demonstrated that satisfactory pressure distribution and heat-flux can be generated by ZONAIR+SHABP (called ZONAIR). Using ZONAIR to generate one set of X-34 aerodynamic/heat rates typically requires *10 minutes on a 550 MHZ PC*, whereas for CFL3D+LATCH it requires 30 hours.

Recent advances in the ZONAIR development are reported. An optimization procedure for TPS weight sizing has been developed using ASTROS optimizer operated on MINIVER by means of an innovative *Complex Variable Differentiation-derived sensitivity*. The result is a *MINIVER/OPT module*. For demonstration, MINIVER/OPT is applied to a prototypical TPS subsystem with a given heat-flux input at point A of X-43. The optimized total TPS weight is then reduced by 30% terminated after the 3<sup>rd</sup> design cycle, while satisfying all TPS temperature constraints. Two types of data mapping procedures have been established. These procedures render *the mappings of aerodynamic forces and temperatures*, through two different interfacing schemes from aerodynamic/panel grid to structural FEM grid, thus allowing the performances of Trim analysis and the aerothermoelastic design of RLV/TPS. Some preliminary results generated by the coupling of AML, a user-oriented automated mesh generator, with ZONAIR demonstrating a 2-body RMLV design process

*The trim solution of the X-34* in terms of the flight loads, input to the structural FEM within ASTROS\*, will yield shear loads and shock loads which will result in strength constraint in the ASTROS\* optimization procedure. Given trajectory inputs, ZONAIR+SHABP aeroheating solution at the nose of X-34 was verified with previous solutions obtained by NASA. *Total optimization loop including the full capacity of ASTROS* will be tested next using an X-34 example as a demonstration case. Further R&D works are recommended to compliment the present ZONAIR/ASTROS program for RLV/TPS design. These include that: i) Further improvement is warranted for ZONAIR to enhance its aerothermodynamics capability in *the high AoA and the lee-side hypersonic flow* regimes, and ii) *A database of TPS material* in terms of their thermal and mechanical properties must be fully established in order to enhance the capability of the optimized scheme.

### **Acknowledgement**

Technical management/advice received from the AFRL monitors Dr. Amarshi Bhungalia and Dr. Jeffery Zweber under U.S. Air Force contract No. F33615-02-C3213 is gratefully acknowledged. Technsoft, Inc. is the subcontractor; ZONA would like to acknowledge the technical effort of Adel Chemaly and Hilmi Kamhawi in AML/ZONAIR integration. The authors thank the technical support rendered by: Mr. David Adamczak of AFRL/VASD (AEROHEAT); Dr. William Wood and Dr. Steven Alter (X-34 Data and Grid Organization); Ms. Katheryn Wurster (MINIVER) of NASA-LaRC; Dr. Christ Riley of CFDesign (LATCH) and Dr. Harry Fuhrmann of Orbital/OSC (X-34 and Data release), during the earlier phase of the present development.

### **References**

1. Freeman D.C., Jr., Talay, T.A., and Austin, R.E., "Reusable Launch Vehicle Technology Program." IAF96-V.4.01, Oct. 1996.
2. Liu, D. D., Chen, P. C., Tang, L., Chang, K. T., Chemaly, A. and Kamhawi, H., "Integrated Hypersonic Aerothermoelastic Methodology for Transatmospheric Vehicle (TAV)/Thermal Protection System (TPS) Structural Design and Optimization," AFRL-VA-WP-TR-2002-3047, January, 2002.
3. Hamilton, H. H., De Jarnette, F. R., and Weilmuenster, K. J., "Approximate Method for Calculating Heating Rates on Three-Dimensional Vehicles," Journal of Spacecraft and Rockets, Vol. 31, No. 3, 1994, pp. 345-354.
4. Chen, P.C. and Liu, D.D. "Unified Hypersonic/Supersonic Panel Method for Aeroelastic Applications to Arbitrary Bodies," Journal of Aircraft, Vol. 39, No. 3, May-June 2002.
5. Johnson, E.H. and Venkayya V.B., "Automated Structural Optimization System (ASTROS), Theoretical, User's, Application's, Programmer's Manual," AFWAL-TR-88-3028, Vol. I-IV, Dec. 1998.

6. "The Adaptive Modeling Language," TECHNOSOFT, Inc., Copyright 1993-1999, [www.technosoft.com](http://www.technosoft.com)
7. Bonner, E., Clever, W., and Dunn, K., "Aerodynamic Preliminary Analysis System II Part I – Theory," NASA CR 182076, Apr. 1991.
8. Hoak, D. E., and Finck, R. D., "USAF Stability and Control Datcom," Vol. 1-4, Air Force Wright Aeronautical Labs., Apr. 1978.
9. Moore, F. G., Mcinville, R. M., and Hymer, T., "The 1998 Version of the NSWC Aeroprediction Code: Part I – Summary of New Theoretical Methodology," NSWCDD/TR-98/1, Apr. 1998.
10. Chen, P.C. and Liu, D.D., "ZONAIR: A Finite-Element Based Aerodynamic/Loads System Using a Unified High-Order Sub/Super/Hypersonic Panel Methodology," Presented at Aerospace Flutter and Dynamics Council, May 8-10, 2002, Sedona, AZ.
11. Engel, C.D., and Schmitz, C.P., "MINIVER Upgrade for the AVID System", Vol. 3, "EXITS User's and Input Guide," NASA CR-172214, Aug. 1983.
12. Krist, S.L., Biedron, R.T., and Rumsey, C.L., "CFL3D User's Manual." NASA Langley Research Center, 1997.
13. Burns, K.A., Deters, K.J., Haley, C.P., Kihlken, T.A., "Viscous Effects on Complex Configurations." WL-TR-95-3059, 1995.
14. Chen, P.C. and Liu, D.D. "Hypersonic Aerodynamic Analysis of Bent-Nose CKEM Body Using ZAERO," Army MRDEC/Dynetics Contract Report (ZONA Rpt 00-40) Oct. 2000.
15. White, F.M., *Viscous Fluid Flow*, McGraw Hill, Inc. 1974.
16. Hamilton, H.H., DeJarnette, F.R., and Weilmuenster, K.J., "Application of Axisymmetric Analogy for Calculating Heating in Three-Dimensional Flows." Journal of Spacecraft, Vol. 24, No. 4, July-August 1987.
17. Myers, D.E., Martin, C.J. and Blosser, M.L., "Parametric Weight Comparison of Advanced Metallic, Ceramic Tile, and Ceramic Blanket Thermal Protection Systems," NASA TM 2000-210289.
18. Lyness JN, Moler, CB, Numerical Differentiation of Analytic Functions, SIAM J. Num. Anal. 4: 202-210, 1967.
19. Chen, P.C., Liu, D.D., Sarhaddi, D., Striz, A.G., Neill, D.J., and Karpel, M., "Enhancement of the Aeroservoelastic Capability in ASTROS," STTR Phase I Final Report, WL-TR-96-3119, Sep. 1996.
20. Chen, P.C., Sarhaddi, D., and Liu, D.D., "Development of the Aerodynamic/ Aeroservoelastic Modules in ASTROS," ZAERO User's/Programmer's/Applications/ Theoretical Manuals, AFRL-VA-WP-TR-1999-3049/3050/3051/3052, Feb. 1999.